

Self-Organized Criticality on Quasiperiodic Graphs

Dieter Joseph

Max-Planck-Institut für Physik komplexer Systeme, Nöthnitzer Str. 38, D-01187 Dresden, Germany

Received: date / Revised version: date

Abstract. Self-organized critical models are used to describe the 1/f-spectra of rather different physical situations like snow avalanches, noise of electric currents, luminosities of stars or topologies of landscapes. The prototype of the SOC-models is the sandpile model of Bak, Tang and Wiesenfeld (Phys. Rev. Lett. **59**, (1987) 381). We implement this model on non-periodic graphs where it can become either isotropic or anisotropic and compare its properties with the periodic counterpart on the square lattice.

PACS. 61.44.Br Quasicrystals – 05.65.+b Self-organized systems

1 Introduction

Self-organized criticality (SOC) is observed in various dynamical systems that develop algebraic correlations. The systems drive themselves into critical states independent of initial states or tuning of parameters. The complex behaviour is characterized by the absence of characteristic time or length scales. It is possible to define a set of critical scaling exponents that characterize the large scale behaviour and describe the universal 1/f-power spectra (for an overview see Ref. 2 in [2]).

Sandpile automata [1] are among the simplest models that develop SOC behaviour in the avalanche propagation. The model is defined as follows: on each site of a lattice, a variable z_i is defined (number of grains of sand). At each time step, the variable at a randomly chosen site is increased $z_i \rightarrow z_i + 1$. Above a critical value z_c , the site topples $z_i \rightarrow z_i - z_c$ and the nearest neighbors j of site i are increased $z_j \rightarrow z_j + 1$. Thereby, z_c grains of sand have been transported from site i to the neighbors j . A toppling can induce nearest neighbor topplings and can create avalanches of arbitrary sizes s . For finite systems, one typically uses open boundary conditions (periodic boundary conditions can lead to never ending avalanches), i.e. the sand is just dropping from the table if it reaches the border. This introduces the concept of finite size scaling (FFS) to compensate cutoff effects. Under the assumption that FFS is valid the avalanches are described by three variables: the number of toppling s , the area a covered by an avalanche and the avalanche duration T . The probability distributions of these variables are algebraic:

$$P(x) = x^{-\tau_x} G\left(\frac{x}{x_c}\right) \quad (1)$$

with $x \in \{s, a, T\}$. G is a cutoff function and the cutoff diverges $x_c \sim L^{\beta_x}$ with the system size $L \rightarrow \infty$. The universality class is determined by the set of exponents

$\{\tau_x, \beta_x\}$. Very recently, the validity of FFS for sandpile models was questioned [3] but this discussion is far beyond the scope of this article. We refer to [3] and references therein and take FFS as a working hypothesis hereafter.

The sandpile automata can be isotropic [1], i.e the sand is distributed equally between nearest neighbors, or anisotropic [4]. The question whether both belong to the same universality class is still under discussion. Whereas real-space normalization group [5], field theoretical [6] and late numerical approaches [2] suggest that both belong to the same universality class, Ben-Hur and Biham [7] question these results.

In what follows we implement the sandpile model on the 8-fold quasiperiodic rhombus-tiling, also called Ammann-Beenker tiling. Due to the specific geometry of quasiperiodic tilings it can become either anisotropic with complete non-deterministic toppling rules, or isotropic with deterministic topplings, or a mixture of both.

2 Non-periodic tilings and SOC

Non-periodic tilings [8] are used to describe the geometry of quasicrystals [9]. They appear in two distinguished classes. The ideal quasiperiodic tilings are produced by a cut-and-project-scheme from a higher dimensional (minimal) embedding lattice [10, 11]. Their vertices are given by so-called model sets [12] and they show pure Bragg-peak diffraction spectra with non-crystallographic symmetries (5,7,8,...-fold). Typically, the tilings are built by two or more prototiles. Fig. 1 shows the 8-fold Ammann-Beenker tiling consisting of two prototiles, a square and a $\pi/4$ rhombus.

The second class of non-periodic tilings are the so-called random tilings. They are constructed by the same prototiles as the ideal ones but this time these prototiles fit together stochastically in such a way that they fill the

entire space, face to face without gaps and overlaps [13, 14]. They also can be embedded into a higher dimensional lattice but their diffraction properties change. They can keep the same symmetry of the ideal counterparts but this time, their diffraction spectrum consists of Bragg-peaks and diffuse scattering (in 3D) or algebraic peaks (in 2D).

Beneath the long-range correlations which govern the diffraction properties, the main difference of non-periodic tilings compared to crystallographic tilings is in their local neighborhood. Whereas we have a fixed translational invariant neighborhood for crystals, we have a finite atlas of different vertex configurations without translational invariance for quasicrystals. For the example of the Ammann-Beenker tiling, we find 6 different vertices in the ideal and 16 different configurations in the random version. The number of nearest neighbors ranges from 3 to 8 [15].

Concerning SOC-models, one now could expect two major influences. Both, long-range correlations and the diversity of the local neighborhoods of the tilings, could develop a difference in the avalanche distribution. It is not necessary to test a lot of different quasiperiodic tilings because the generic features of quasiperiodicity are the same. Symmetry or the type of the tiling plays a minor rôle. Additionally, the local configurations allow different implementations of e.g. the sandpile model. For simplicity we will focus on three potentially different versions (there are more possible but typically they fall in the same categories) on the 8-fold Ammann-Beenker tiling:

- (I) anisotropic and non-deterministic: The critical height z_c and the number of toppling grains $n_i = z_c > 0$ are equal for all vertices i of the tiling. At every toppling step one has to make a random choice to distribute the n_i grains among the N_i neighbors ($3 \leq N_i \leq 8$) of the toppling vertex i .
- (II) partly isotropic and deterministic, partly not: z_c is equal for all vertices i but greater or equal to the minimal number of neighbors $N_{\min} = 3$ and less than the maximal number of neighbors $N_{\max} = 8$. The number of topplings at site i is $n_i = \min(z_c, N_i)$ where N_i again is the number of neighbors of vertex i . This way, the toppling rules are locally isotropic and deterministic for vertices with $N_i \leq z_c$ but anisotropic and non-deterministic for all the others because of the random choice one has to make in order to distribute the $n_i = z_c$ grains among the $N_i > z_c$ neighbors.
- (III) isotropic and deterministic: z_c is greater or equal than the maximal number of neighbors $N_{\max} = 8$, but the number of toppling grains of vertex i is always $n_i = N_i$. This way, every bond will transport the same amount of grain in both directions and the number of topplings is given locally by the number of neighbors.

After a suitable thermalization, we perform $2 * 10^6$ ($L = 16, 32, 64$) and $5 * 10^5$ ($L = 128, 256$) avalanches for the different scenarios. Each avalanche is separated by an appropriate thermalization time to prevent cross-correlations. The system size ($L \times L$) is given by the length L which varies from 16 to 256 whereas the absolute scale is

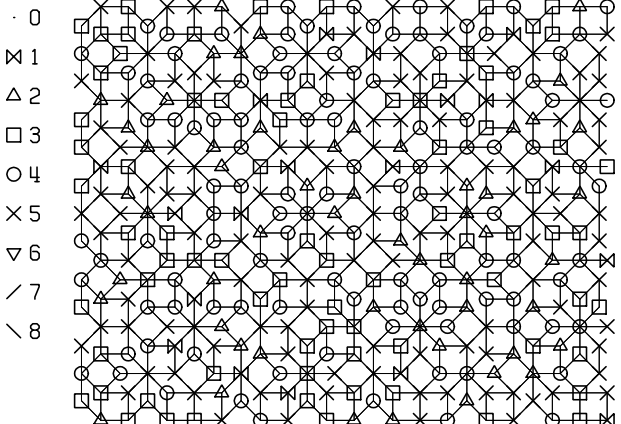


Fig. 1. The ideal Ammann-Beenker tiling and a critical state at the end of an avalanche of type **(I)**. The symbols on top of the vertices code the number of grains of sand z_i and $z_c = 5$.

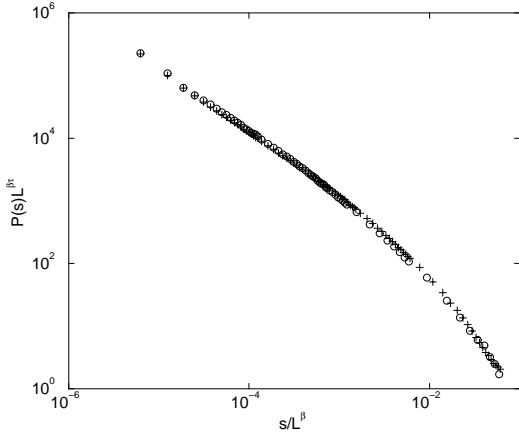


Fig. 2. Comparison of anisotropic avalanche distributions of an ideal and a random tiling version of the Ammann-Beenker tiling at $L=128$.

given by the bond length of the tiling that is equal to one. For each setting, the avalanche distributions are stored. According to the finite size scaling assumption, the data for the different length scales should collapse to a single curve that is determined by the critical exponents τ_x, β_x . Fig. 3 shows the data collapse of the probability distributions of the number of topplings s for version **(I)**, Fig. 4 for version **(II)**, and Fig. 5 for the isotropic deterministic version **(III)**. Table 1 gives the extracted numerical values for the exponents. The errors given in the brackets are the statistical errors of the fitting procedure.

Within the limits set by the small statistic, all three versions belong to the same universality class: the critical exponents and also the scaling functions seem to be the same. If one compares the distributions of the ideal quasiperiodic tilings and the corresponding random tiling, there is no apparent difference (see Fig. 2). Looking at the crystalline counterpart, the 2D square lattice, the state of the art values for the exponents are $\tau_s = 1.27(1)$ and $\beta_s = 2.73(2)$ [2]. These values are determined by massive parallelized computation. From the difference to Table 1

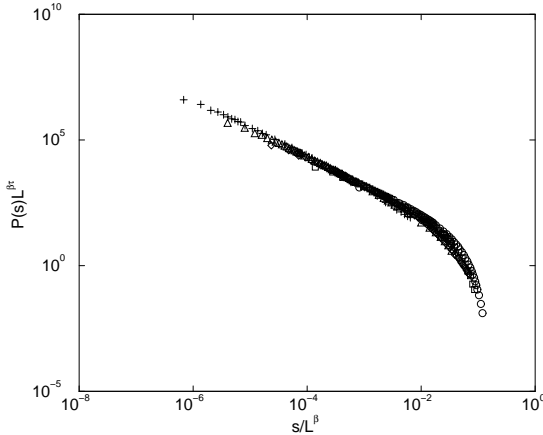


Fig. 3. Data Collaps of the probability distribution of the number of topplings s for the anisotropic, non-deterministic version (I) on the ideal Ammann-Beenker tiling. System lengths are $L=16$ (○), 32 (□), 64 (◇), 128 (△), and 256 (+).

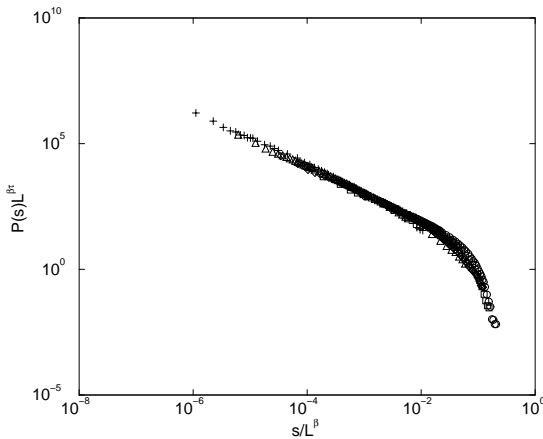


Fig. 4. Data Collaps of the probability distribution of the number of topplings s for version (II) on the ideal Ammann-Beenker tiling. System lengths and symbols as in Fig. 3.

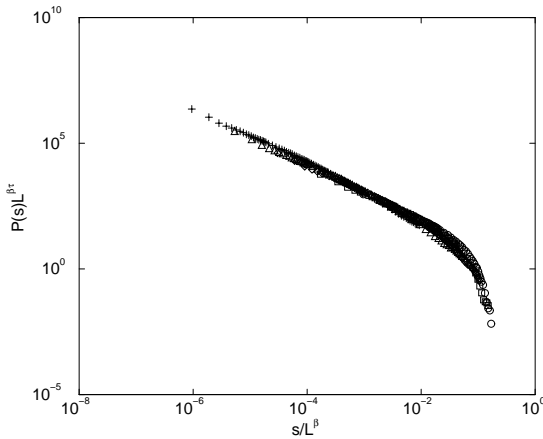


Fig. 5. Data Collaps of the probability distribution of the number of topplings s for the isotropic, deterministic version (III) on the ideal Ammann-Beenker tiling. System lengths and symbols as in Fig. 3.

Table 1. The critical exponents τ_s, β_s of the three tested versions (Statistical errors are given in brackets).

| | Version (I) | Version (II) | Version (III) |
|-----------|-------------|--------------|---------------|
| τ_s | 1.20(3) | 1.19(3) | 1.19(3) |
| β_s | 2.5(2) | 2.5(2) | 2.5(2) |

one cannot conclude that there exists a different universality class for quasiperiodic graphs. The values of Table 1 are more comparable to older estimates for the square lattice based on similar statistics [16]. The distributions for the area a and duration T are not shown because they behave in the same way.

3 Conclusion

We have performed numerical estimates of the critical exponents of the 2D sandpile model on the 8-fold quasiperiodic Ammann-Beenker tiling. Thereby, three different version (anisotropic-non-deterministic, isotropic-deterministic and a mixed one) were implemented on the ideal and on the random Ammann-Beenker tiling. The measured exponents are comparable to early numerical results of the 2D square lattice and might suggest that all tested version belong to the same universality class as the 2D square lattice. The problem however remains to substantiate this, e.g. by better statistics. This can only be achieved by a massive use of a parallel computing which is not at hand at the moment. But the situation seems to be similar to the investigation of Ising-models [17] which led to the conclusion that aperiodic and periodic versions belong to the same universality class.

The author wants to thank S. Maslov and M. Baake for discussion and helpful comments.

References

1. P. Bak, C. Tang and K. Wiesenfeld, Phys. Rev. Lett. **59**, (1987) 381, Phys. Rev. A **38**, (1988) 364.
2. A. Chessa et al., Phys. Rev. E **59**, (1999) R12.
3. B. Drossel, cond-mat/9904075 v2
4. S. S. Manna, J. Phys. A **24**, (1991) L363.
5. L. Pietronero, A. Vespignani, and S. Zapperi, Phys. Rev. Lett. **72**, (1994) 1690.
6. R. Dickman, A. Vespignani, and S. Zapperi, Phys. Rev. E **57**, (1998) 5095.
7. A. Ben-Hur and O. Biham, Phys. Rev. E **53**, (1996) R1317.
8. G. Grünbaum and C. Shepard, *Tilings and Patterns* (W. H. Freeman, New York 1987).
9. D. Shechtman et al., Phys. Rev. Lett. **53**, (1984) 1951.
10. P. Kramer and R. Neri, Acta Cryst. A **40**, (1984) 580.
11. M. Baake et al. J. Phys. A: Math. Gen. **23**, (1990) L1037.
12. R. V. Moody, *The Mathematics of long-range order*, ed. R. V. Moody, NATO ASI Series C489 (Kluwer, Dordrecht 1997) 403.
13. V. Elser, Phys. Rev. Lett. **54**, (1985) 1730.

14. C. L. Henley in, *Quasicrystals: The State of the Art*, eds. D. P. DiVincenzo and P. J. Steinhardt, (World Scientific, Singapore 1991) 429.
15. M. Baake and D. Joseph, Phys. Rev. B **42**, (1990) 8091.
16. P. Grassberger and S. S. Manna, J. Phys. (France) **51** (1990) 1077.
17. J. Hermisson, U. Grimm and M. Baake, J. Phys. A: Math. Gen. **30**, (1997) 7315.